Received: 8 May 2020 | Revised: 27 July 2020 | Accepted: 9 August 2020

DOI: 10.1111/ffe.13336

ORIGINAL CONTRIBUTION

FFEMS Fatigue & Fracture of Engineering Materials & Structures WILEY

Fatigue assessment of high strength welded joints through the strain energy density method

Pietro Foti | **Filippo Berto**

Mechanical and Industrial Engineering (MTP), Norwegian University of Science and Technology, Trondheim, Norway

Correspondence
Pietro Foti, Mechanical and Industrial Engineering (MTP), Norwegian University of Science and Technology, Richard Birkelands vei 2B, Trondheim 7491, Norway.
Email: pietro.foti@ntnu.no

Funding information
European Union's Horizon 2020 research and innovation programme, Grant/Award Number: 764011

Abstract

The main aim of the present work is to investigate, through the strain energy density method, the fatigue behaviour of high strength welded joints realised employed in hydraulic runner blades. The geometries, found in literature, present the welding bead machined in order to have no geometrical discontinuities in the specimen realising a wide fitting radius between the two welded plates; the only critical geometrical discontinuity in the specimen is given by the lack of penetration that leads to an internal crack-like defect. The specimens presented failure both from the weld toe and from the weld root depending on the amount of welding penetration. The results, summarised in this work with the strain energy density method, show clearly the possibility to consider a unique master curve for this kind of joints regardless of the failure initiation point. Acquiring, through a finite element model, the strain energy density value both at the weld toe and at the weld root and comparing them, the method is proved to be adequate to detect the most critical area of the joint. A first fatigue master curve in terms of cyclic averaged strain energy density value is provided for the fatigue design of high strength welded joints.

KEYWORDS

fatigue design, high strength steels, strain energy density, turbine blade component

1 | INTRODUCTION

The welded joints between the blades and the band or crown of a Francis turbine runner can be idealised by a simple rounded T-joint subject to bending loading condition. Due to the considerable thickness of the components welded together, the joint is often realised with a partial penetration, resulting in an internal crack-like defect within the welded component.[1–3] The presence of a crack, however, does not mean that the crack has to represent the critical point of the component relatively to structural integrity and fatigue failure as a matter of fact. As reported in some works,[1,4–6] available in literature, the failure can initiate from different locations, depending on the component geometry and loading condition. This leads to the need of valid methods to assess the fatigue life of the component, but also able to evaluate the most likely material point from that failure is expected to initiate.

The most used method for fatigue design of welded components is the nominal stress method,[7–9] that considers external loads or nominal stresses in the critical cross-section and compares them with the S-N curves that correlate the fatigue strength with the number of cycles. However, this approach results to be impractical for the purposes stated above, and its use is limited by the geometry and loading conditions of specimens reported in common standards curve.[7–9]

Besides, the nominal stress method does not allow direct comparisons between the weld root and the weld toe whose fatigue failure must be assessed through two different fatigue master curves. Indeed, dealing with some similar cases, like the cruciform welded joint with incomplete penetration, subjected to a tensile loading on the attached plate, the standards suggest to perform the fatigue assessment both at the weld toe and at the weld root using two different fatigue master curves and taking into account, respectively, the nominal stress in the attached plate and the nominal stress in a particular section of the weld bead resulting in a very conservative design.[9]

On the other hand, the so-called local approaches allow a more realistic evaluation of the expected fatigue life.[10–16] In particular, among them, the authors consider in the present work the strain energy density (SED) method that, unlike other local approaches, like the notch stress intensity factor (NSIF) method, that allows to estimate the failure modes like, for example, weld root failure or weld toe failure.[17] In the present work, some experimental fatigue tests,[1] carried out for the fatigue assessment of turbine runners, are analysed through the SED method in order to evaluate the accuracy of SED method in estimation of failure mode.

2 | SED METHOD AND TESTS EXAMINED

2.1 | SED method

The SED method is an energetic local approach proved as a method to investigate both fracture failure in static condition and fatigue failure.[18–25]

Regarding the static condition, the method makes the assumption that the brittle fracture occurs when the local SED, $\bar{W}$, averaged over a given control volume, reaches a critical value, that is $\bar{W}=W_C$ that results to be independent on both the local geometry and the loading mode.[18,19,26] Dealing with an ideally brittle material under static conditions, the SED critical value can be evaluated through the conventional ultimate tensile strength,σ_t, and the Young's modulus of the material:

$$W_C=\frac{\sigma_t^2}{2E}. \tag{1}$$

What stated above represents the basic idea of this method, whose analytical frame[27–29] demonstrates also connections in closed form solutions with other fracture mechanics methods such as the notch stress intensity factor one.

Even if, as stated above, the SED critical value results to be independent on both the local geometry and the loading type, this is not true for the control volume used for its computation, but it takes different shapes, with regard of the local geometry, and different positions, according to the loading mode.

By considering blunt notches,[30–40] some considerations must be done about the control volume that assumes a crescent shape, with R_0 being its maximum depth inside the component. The control volume is given by the intersection between the component and a circle with radius r+R_0, which centre is not always located on the notch bisector, but also on a line rigidly rotated with respect to it and centred on that point where the SED reaches its maximum value (Figure 1). The centre of this circle is located between the notch edge and the notch-fitting radius centre at a distance r, from the notch edge, as shown in Figure 1B,C, for rounded V-notches, and in Figure 1E,F, for U-notches.

By considering welded joints made of steel or aluminium,[39,41–43] two conditions allow the use of the SED method to assess their high cycle fatigue properties in terms of the cyclic average SED, $\Delta\bar{W}$: the brittle nature of the failure and the fact that it happens under linear elastic regime.

The material properties, in the vicinity of the weld toe and root, depend on several parameters such as residual stresses, heterogeneous metallurgical microstructures, distortions, defects, inclusions and weld thermal cycles. If all these welding peculiarities had to be taken into account specifically, of course, the use of the SED approach would have some complications; however, in order to match the user need of a realistic evaluation of the fatigue strength with a relatively simple approach, all the welding peculiarities effects are treated in a statistical way by considering only the geometry of the component. Under such an assumption, the material parameter R_0 can be estimated by means of the following expression[18]:

$$R_0=\left(\frac{\sqrt{2e_1}\Delta K_{1A}^N}{\Delta\sigma_A}\right)^{\frac{1}{1-\lambda_i}}, \tag{2}$$

where $\Delta\sigma_A$ is the fatigue strength of the butt ground welded joint, taking into account the influence of the welding process in the lack of any stress concentration effect, ΔK_{1A}^N is the NSIF-based fatigue strength of the welded joint having a V-notch angle at the weld toe constant and large enough to ensure the non-singularity of

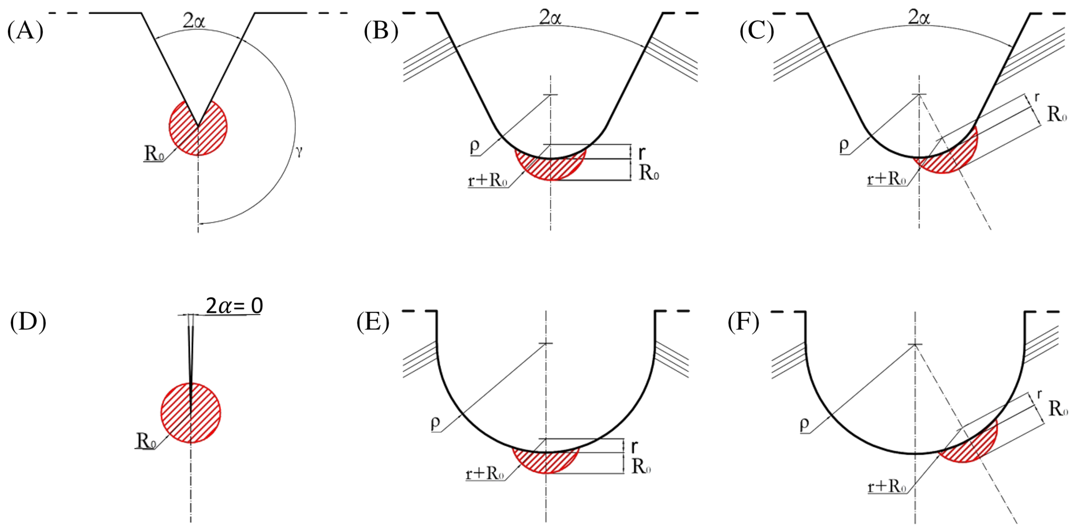

FIGURE 1 Control volume for (A) sharp V-notch; (B) blunt V-notch under mode I loading ($r=\rho\cdot(\pi-2\alpha)/(2\pi-2\alpha)$); (C) blunt V-notch under mixed mode loading ($r=\rho\cdot(\pi-2\alpha)/(2\pi-2\alpha)$); (D) crack; (E) U-notch under mode I loading ($r=\rho/2$) and (F) U-notch under mixed mode loading ($r=\rho/2$) [Colour figure can be viewed at wileyonlinelibrary.com]

mode II stress contribution and λ_1 and e_1 are parameters depending on the V-notch opening angle.

Knowing the fatigue master curve in terms of mean SED, it is possible to evaluate the fatigue strength in terms of stress amplitude; it is enough to calculate the mean-SED at the weld toe or root for a generic remote tensile load $\Delta\sigma_1$ through a static finite element (FE) simulation and, by means of Equation 3, valid only under the assumption of linear elastic behaviour, the fatigue strength of the component in terms of stress amplitude, $\Delta\sigma_L$, can be evaluated exploiting the following equation:

$$\Delta\sigma_L=\Delta\sigma_i\left(\frac{\Delta\bar{W}_L}{\Delta\bar{W}_i}\right)^{\frac{1}{2}}, \tag{3}$$

being $\Delta\bar{W}_L$ the averaged SED value at $2\cdot10^6$ loading cycles.

In order to assess the fatigue life of a components employing the SED method, once the SED value $\Delta\bar{W}$ is known for the loading conditions considered, it is possible to apply the following equation:

$$N_f=\left(\frac{\Delta\bar{W}_L}{\Delta\bar{W}}\right)^k\cdot 2\cdot10^6, \tag{4}$$

being k the inverse slope of the fatigue master curve, plotted in a double logarithmic diagram and reporting the averaged SED, $\Delta\bar{W}$, versus the number of cycles to failure, N_f.

2.2 | Data from literature

Dealing with fatigue failure of steel welded joint realised through common welding techniques, the first validation of the SED method was performed by considering an experimental campaign carried out on more than 300 fatigue data with toe failure under different loading modes.[39] The analysis was completed by considering other experimental data,[41] involving components with failure both from weld toe and root, under different loading modes, providing a final synthesis based on 900 experimental data,[27,41,44] where for such tests the number of cycles to failure is given as a function of the cyclic average SED, $\Delta\bar{W}$, in Figure 2.

The purpose of the present work is to determine the scatter band in terms of cyclic averaged SED, of experimental data available in literature,[1] with regards to high strength welded joints, commonly used in turbine runner application, in order to provide a valid tool to assess the fatigue properties of this kind of component.

The welded joints between blades and band/crown of a Francis turbine runners can be idealised by a T-joint, with a large fillet between the two plates, subjected to bending load condition. In the present work, some fatigue data, found in literature[1] related to such joints, are analysed. The specimens, whose geometry is shown in Figure 3, were made of two plates of AISI415 whose cast version, the CA6NM grade, is usually employed in hydraulic turbine industry. The specimens were made by multipass flux core arc welding (FCAW), that is an arc welding process, that uses a continuous flux-cored filler

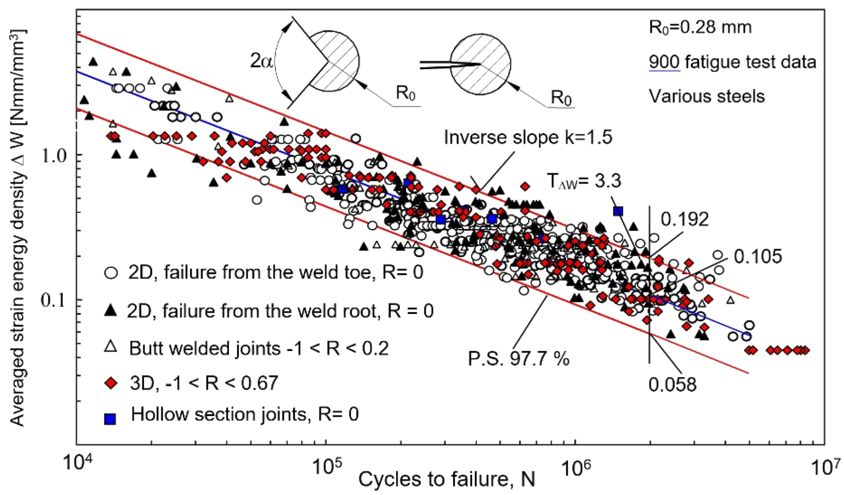

FIGURE 2 Fatigue strength of steel welded joints as a function of the averaged local strain energy density[44] [Colour figure can be viewed at wileyonlinelibrary.com]

wire. The welding electrodes were made of E410NiMo for the A, B and C series specimens listed in Table 1. The weld metal E410NiMo is a martensitic stainless steel with a good weldability and a chemical composition matching that of AISI415 base metal. Anyway, the welding with this martensitic metal required a preheat of the base material at a temperature of 100 ° C, in order to prevent hydrogen cracking and to reduce the shrinkage stresses. For the D and E series specimens, listed in Table 1, another weld metal was used for the first welding pass, that is, a E316L austenitic stainless steel that does not require preheating. Each specimen was precracked as shown in Figure 3. Considering the different initial crack length, 2a, realised and the need to have enough material for the weld toe grinding, performed to round the corners at the weld toes like in the fabrication of turbine runners, the different specimens series required different number of welding passes with this number increasing with decreasing the initial crack length requiring a deeper welding for the component. The welded assemblies, at the end of the process, were also tempered by slow heating to 595 ° C, holding for 5 h and slow air-cooling to the room temperature, bringing also a stress-relieving effect to the weld.

Table 1 reports the principal parameters and the results of the fatigue tests available in the literature and reanalysed in the present work in terms of averaged SED.

3 | FE ANALYSIS

In order to summarise the fatigue data available in literature[1] in terms of averaged SED, $\Delta\bar{W}$, the specimen geometry reported in Figure 3 is modelled through the software Ansys APDL[45] carrying out a static analysis (Ansys APDL command ANTYPE set to 0) by adopting a mapped mesh pattern consisting of 2D, second-order, eight node, square plane elements (PLANE 183 of Ansys element library with K-option 1 set to 1) considered in plane strain condition (K-option 3 set to 2). The element size utilised in the model goes from one eighth of the control volume radius, $R_0 = 0.2$ mm, at the weld root vertex and at the weld toe critical point, to one eighth of the plates thickness, $t = 33$ mm.

The application of the SED method to the component analysed in the present work requires two

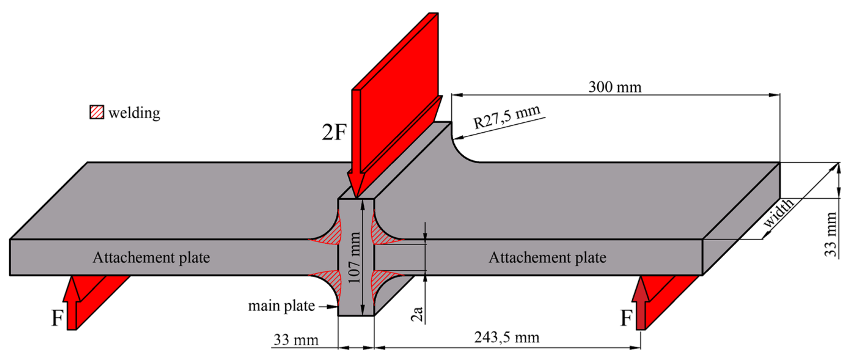

FIGURE 3 Specimen geometry and loading conditions [Colour figure can be viewed at wileyonlinelibrary.com]

TABLE 1 Fatigue tests data from literature[1]

Series	Welding metal	Width (mm)	Initial crack length 2a (mm)	Failure	Failure initiation point	σ_{an} (MPa)	Number of cycles to failure
A	E410NiMo (all passes)	100	7	Yes	Toe	702	159 416
				Yes	Toe	702	168 985
				Run-out	—	702	496 824
				Yes	Toe	621	315 307
				Yes	Toe	540	1 078 727
				Run-out	—	459	7 920 164
B	E410NiMo (all passes)	100	12	Yes	Toe	702	135 408
				Yes	Root	621	222 247
				Yes	Root	540	468 690
				Yes	Root	459	1 143 478
				Run-out	—	378	2 773 563
C	E410NiMo (all passes)	100	16	Yes	Root	702	47 419
				Yes	Root	702	51 152
				Yes	Root	621	66 108
				Yes	Root	540	114 348
				Yes	Root	459	188 777
				Yes	Root	378	447 335
D	E316L (first pass) E410NiMo (other passes)	100	16	Yes	Root	702	33 423
				Yes	Root	540	87 452
				Yes	Root	378	236 965
				Yes	Root	300	542 222
				Yes	Root	340	1 177 297
E	E316L (first pass) E410NiMo (other passes)	35	16	Yes	Root	225	2 121 203
				Run-out	—	207	8 250 033

different numerical simulations. Regarding the weld toe, a first simulation is needed in order to define the material point of maximum of the first principal stress field along the notch fillet, whose position represent the input for a second simulation performed to build the control volume as shown in Figure 1C. Dealing with the weld root, that is modelled as a sharp V-notch, the control volume position is already known and must be treated as in Figure. 1D.

In order to obtain a more efficient analyses and minimise the computational time, the symmetries of the component examined are exploited, by using 2D models for each simulation by implementing suitable symmetry conditions in the FE model, as shown in Figure 4 for the first of the two models needed to apply the SED method to this kind of components.

4 | RESULTS AND DISCUSSIONS

In the range of cycles considered, no change in the material behaviour has been noticed in the data analysed that could suggest a failure in the low cycle fatigue regime. As regards the specimens analysed in the present work, the nominal stress method leads to different fatigue master curve with changing the length of the internal crack in the component and the material point where the failure began (weld root or weld toe) as it is shown in Figure 5.

In order to apply the SED method, the averaged SED value, $\Delta\bar{W}$, is evaluated in a given control volume, as described in Section 2.1, by using a static FE analysis and applying to the model the maximum value of the load reached during the fatigue tests considered.

It is worth underlining that the weldments under consideration have a higher strength with respect to

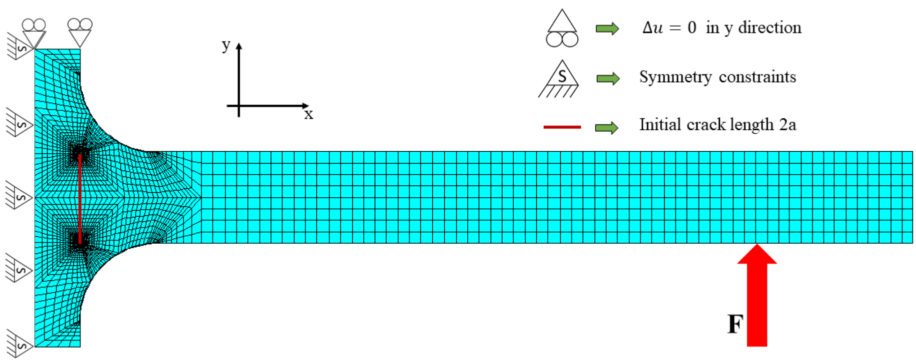

FIGURE 4 Two-dimensional finite element model and loading conditions of the component analysed [Colour figure can be viewed at wileyonlinelibrary.com]

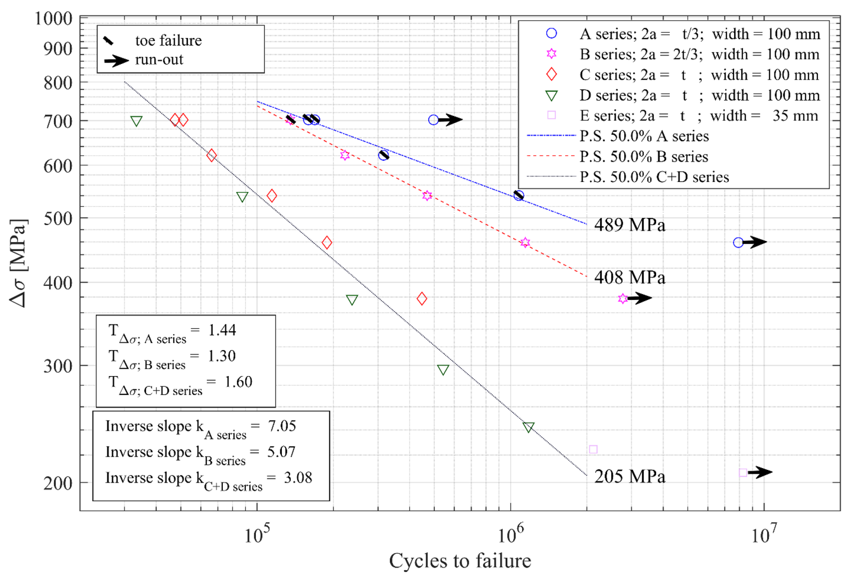

FIGURE 5 $\Delta\sigma$ versus number of cycles to failure double logarithmic diagram for high steel welded joints with competing failure modes, from weld toe and weld root, with linear interpolation of the data considering probabilities of survival of $P.S = 50\%$ [Colour figure can be viewed at wileyonlinelibrary.com]

those realised with common welding techniques,[46] leading to the need of a different fatigue curve for this kind of weldments with respect to those considered by the standards.[46] The higher fatigue performance of these weldments becomes clear by comparing the NSIF-based fatigue strength at $5 \cdot 10^6$ cycles of welded joints made of structural steels,[10,27] and equal to $\Delta K_{th} = 180\,\text{MPa}\sqrt{\text{mm}}$, with that evaluated for the specimens under consideration,[1] and equal to $\Delta K_{th} = 215\,\text{MPa}\sqrt{\text{mm}}$.

The use of the control volume radius, usually adopted dealing with common steel welded joints,[39] has been proved to be inadequate for assessing the fatigue properties of high-performing welded joints.[46] The adopted control volume radius is equal to $R_0 = 0.2$ mm that results to be optimal in describing the higher fatigue performance of these weldments.

The same considerations are possible also by comparing the SED scatter band for weldments realised with classic welding techniques, shown in Figure 2, with those analysed in the present section, as it is shown in Figure 6; more precisely, the better performances of the high strength welded joint are clear comparing the SED master curve values at $2 \cdot 10^6$ cycles.

It is not possible to compare, in terms of nominal stress, the welded component analysed in this work with components having the same geometry but realised through common welding technique not having suitable experimental data available to carry out such a comparison; however, through the SED method, it is possible to estimate the fatigue strength in terms of nominal stress for the butt ground welded joint, exploiting the following equation:

$$\Delta\bar{W} = \frac{\Delta\sigma^2}{2E}, \tag{5}$$

by assuming a Young's modulus $E = 200\ 000$ MPa and the fatigue master curve in terms of averaged SED, $\Delta\bar{W}$, reported in Figure 6, it is possible to obtain for the butt ground welded joint an approximate value of $\Delta\sigma = 315$ MPa at $5 \cdot 10^6$ cycles, whereas $\Delta\sigma$ for weldments made through common welding techniques is

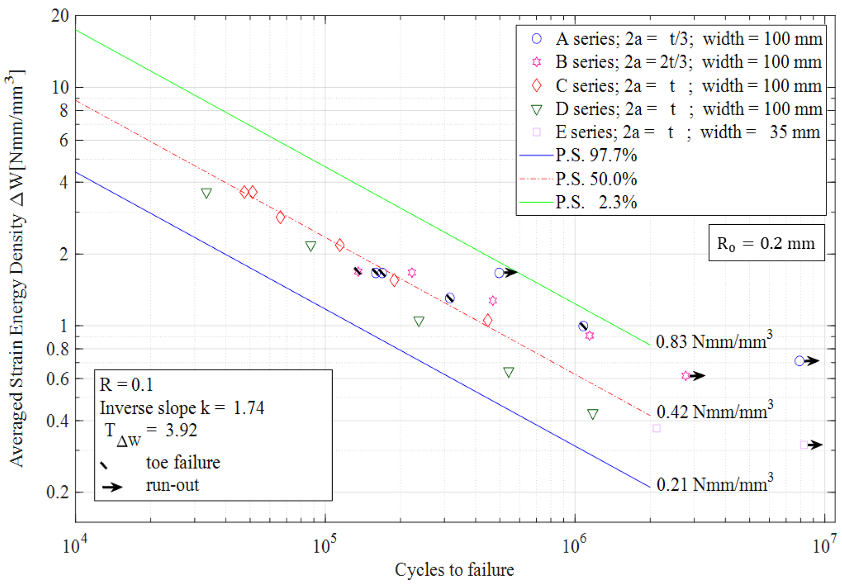

FIGURE 6 $\Delta\bar{W}$ versus number of cycles double logarithmic diagram for high steel welded joints with competing failure modes, from weld toe and weld root with linear interpolation of the data considering probabilities of survival of $P.S = 97.7\%$, $P.S = 50\%$ and $P.S = 2.3\%$ [Colour figure can be viewed at wileyonlinelibrary.com]

$\Delta\sigma = 155$ MPa.[10,27] The use of Equation 5 to carry out the considerations above is appropriate considering that in the high cycle regime, the fatigue failure in the components results to be brittle and under linear elastic regime.

As regards the fatigue data analysed, which involve specimens with competing fatigue failure modes, from weld toe and weld root, it is possible to notice, from the diagram reported in Figure 6, that the SED method is able to consider these kind of failures through a unique fatigue master curve with a narrow scatter band characterised by a scatter index equal to $T_{\Delta W} = 3.92$. Besides, in order to have a proper comparison with the nominal stress method, it is worth underlining that the scatter index, reconverted to an equivalent local stress range,[44] is equal to $T_{\Delta\sigma} = \sqrt{T_{\Delta W}} = 1.98$. In addition, the method allows to determine the most critical point of the component even with a complex geometry as the one reported in Figure 3 that, depending on the initial crack length, 2a, could experience both failure from weld root and weld toe. Indeed, as regards the specimens of A series, $\Delta\bar{W}_{toe} \approx 1.75 \cdot \Delta\bar{W}_{root}$, indicating that the most likely point for the origin of the fatigue failure for these specimens is the weld toe; as regards the specimens of B series, $\Delta\bar{W}_{toe} \approx 0.80 \cdot \Delta\bar{W}_{root}$ indicating failure from the weld root; as regards the specimens of C, D and E series, $\Delta\bar{W}_{toe} \approx 0.47 \cdot \Delta\bar{W}_{root}$, indicating failure from the weld root.

The experimental data are in good agreement with the SED method estimations with the exception of one specimen of the B series, that presents toe failure instead of root failure as expected; according to the authors, considering that for this particular geometry the SED value at the weld toe and at the weld root are almost the same, the specimen that presented failure from the weld toe had a geometry that deviates slightly from that reported in literature,[1] that is, shorter initial crack length or a pre-existing defect at the weld toe, resulting in a more critical condition for the weld toe.

5 | CONCLUSIONS

The possibility to apply the SED method to assess the fatigue life of high strength welded joints as those employed in Francis turbine runner applications has been verified. Experimental data from literature, represented by welded joints of turbine runners, have been summarised through the SED method in order to obtain a fatigue master curve and to assess the critical point of the component that leads to fatigue failure. The specimens analysed showed fatigue failure modes depending on the weld penetration depth. The main conclusions are the following:

- The SED method provides a good assessment of the origin of fatigue failure in accordance with the experimental data;
- The SED method manages to summarise in a unique fatigue master curve, with a narrow scatter band, fatigue results characterised by competing failures that are both at weld toe and weld root.
- Dealing with high strength welded joints analysed, a small control volume radius, $R_0 = 0.2$ mm, must be used, rather than $R_0 = 0.28$ mm as suggested dealing with common welding techniques.
- The comparison between the fatigue strength at $5 \cdot 10^6$ cycles in terms of stress of butt ground welded joints and that related to the specimens analysed in the

present work, that is $\Delta\sigma = 315$ MPa against $\Delta\sigma = 155$ MPa, respectively, highlights good fatigue performance of the method of this kind of weldments.

ACKNOWLEDGEMENT

The work presented in this paper has received funding from the European Union's Horizon 2020 research and innovation programme under Grant agreement 764011.

NOMENCLATURE

e_1	mode 1 function in the SED expression for sharp V-notches. Available in literature
E	Young's modulus
K_{IC}	material toughness
N_f	Number of cycles to failure
R_0	radius of the control volume
r	geometrical parameter defining the control volume shape for blunt notches
SED	strain energy density
T	component plates thickness
W_C	critical strain energy density value
$\bar{W}$	averaged strain energy density value
ΔK_{1A}^{N}	NSIF-based fatigue strength for V-notches with $2\alpha \neq 0^{\circ}$
ΔK_{th}	weld root NSIF-based fatigue strength.
$\Delta\bar{W}$	cyclic averaged strain energy density value
$\Delta\bar{W}_i$	generic cyclic averaged strain energy density value for a remote tensile load $\Delta\sigma_i$
$\Delta\bar{W}_L$	component fatigue strength in terms of cyclic averaged strain energy density value
$\Delta\bar{W}_{root}$	cyclic averaged strain energy density value at the weld root
$\Delta\bar{W}_{toe}$	cyclic averaged strain energy density value at the weld toe
$\Delta\sigma_A$	butt ground welded joint fatigue strength
$\Delta\sigma_i$	generic remote tensile load.
$\Delta\sigma_L$	component fatigue strength
λ_1	mode I Williams' eigenvalues for stress distribution at V-notches
ν	Poisson's ratio
σ_t	conventional ultimate tensile strength
2α	opening angle of V-notch

ORCID

Pietro Foti https://orcid.org/0000-0003-2852-7560
Filippo Berto https://orcid.org/0000-0001-9676-9970

REFERENCES

1. Ghafoori-Ahangar R, Verreman Y. Fatigue behavior of load-carrying cruciform joints with partial penetration fillet welds under three-point bending. *Eng Fract Mech*. 2019;215:211-223.
2. Carpinteri A, Brighenti R, Huth HJ, Vantadori S. Fatigue growth of a surface crack in a welded T-joint. *Int J Fatigue*. 2005;27(1):59-69.
3. Vantadori S, Carpinteri A, Scorza D. Simplified analysis of fracture behaviour of a Francis hydraulic turbine runner blade. *Fatigue Fract Eng Mater Struct*. 2013;36(7):679-688.
4. Kainuma S, Mori T. A study on fatigue crack initiation point of load-carrying fillet welded cruciform joints. *Int J Fatigue*. 2008;30(9):1669-1677.
5. Dong Y, Guedes Soares C. *On the Fatigue Crack Initiation Point of Load-Carrying Fillet Welded Joints*. London, UK: Towar Green Mar Technol Transp Taylor Fr Group; 2015:406-407.
6. Balasubramanian V, Guha B. Establishing criteria for root and toe cracking of load carrying cruciform joints of pressure vessel grade steel. *Eng Fail Anal*. 2004;11(6):967-974.
7. Fricke W. IIW guideline for the assessment of weld root fatigue. *Weld World*. 2013;57(6):753-791.
8. B. E. 1993-1-3:2009, “Eurocode 3: design of steel structures—part 1–9: fatigue,” in *Eurocode 3: Design of Steel Structures—Part 1–9: Fatigue*, 2011, vol. 7, no. 2006.
9. Hobbacher A. IIW document IIW-1823-07 Fatigue Design of Welded. 2008.
10. Radaj D, Sonsino CM, Fricke W. *Fatigue Assessment of Welded Joints by Local Approaches*. Second ed. ; 2006.
11. Carpinteri A, Boaretto J, Fortese G, et al. Fatigue life estimation of fillet-welded tubular T-joints subjected to multiaxial loading. *Int J Fatigue*. 2017;101:263-270.
12. Vantadori S, Boaretto J, Fortese G, et al. Fatigue strength of welded joints under multiaxial non-proportional loading. *Procedia Struct Integr*. 2017;5:761-768.
13. Song W, Liu X, Razavi SMJ. Fatigue assessment of steel load-carrying cruciform welded joints by means of local approaches. *Fatigue Fract Eng Mater Struct*. 2018;41(12):2598-2613.
14. Macek W, Łagoda T, Mucha N. Energy-based fatigue failure characteristics of materials under random bending loading in elastic-plastic range. *Fatigue Fract Eng Mater Struct*. 2018;41(2):249-259.
15. Lepore MA, Maligno AR, Berto F. Crack closure in friction stir weldment using non-linear model for fatigue crack propagation. *Fatigue Fract Eng Mater Struct*. 2019;42(11):2596-2608.
16. Colussi M, Ferro P, Berto F, Meneghetti G. The peak stress method to calculate residual notch stress intensity factors in welded joints. *Fatigue Fract Eng Mater Struct*. 2018;41(4):727-738.
17. Radaj D, Sonsino CM, Fricke W. Recent developments in local concepts of fatigue assessment of welded joints. *Int J Fatigue*. 2009;31(1):2-11.
18. Lazzarin P, Zambardi R. A finite-volume-energy based approach to predict the static and fatigue behavior of components with sharp V-shaped notches. *Int J Fract*. 2001;112(3):275-298.
19. Lazzarin P, Zambardi R. The equivalent strain energy density approach re-formulated and applied to sharp V-shaped notches under localized and generalized plasticity. *Fatigue Fract Eng Mater Struct*. 2002;25(10):917-928.
20. Lazzarin P, Livieri P, Berto F, Zappalorto M. Local strain energy density and fatigue strength of welded joints under

uniaxial and multiaxial loading. *Eng Fract Mech.* 2008;75(7):1875-1889.
21. Berto F, Gallo P, Lazzarin P. High temperature fatigue tests of un-notched and notched specimens made of 40CrMoV13.9 steel. *Mater Des.* 2014;63: 609–619.
22. Razavi SMJ, Ferro P, Berto F, Torgersen J. Fatigue strength of blunt V-notched specimens produced by selective laser melting of Ti-6Al-4V. *Theor Appl Fract Mech*. 2018;97:376-384.
23. Aliha MRM, Berto F, Mousavi A, Razavi SMJ. On the applicability of ASED criterion for predicting mixed mode I+II fracture toughness results of a rock material. *Theor Appl Fract Mech.* 2017;92:198-204.
24. Torabi AR, Campagnolo A, Berto F. Local strain energy density to predict mode II brittle fracture in Brazilian disk specimens weakened by V-notches with end holes. *Mater des*. 2015;69:22-29.
25. Berto F, Barati E. Fracture assessment of U-notches under three point bending by means of local energy density. *Mater des.* 2011;32(2):822-830.
26. Lazzarin P, Berto F, Gomez FJ, Zappalorto M. Some advantages derived from the use of the strain energy density over a control volume in fatigue strength assessments of welded joints. *Int J Fatigue.* 2008;30(8):1345-1357.
27. Berto F, Lazzarin P. Recent developments in brittle and quasi-brittle failure assessment of engineering materials by means of local approaches. *Mater Sci Eng R Reports*. 2014;75:1-48.
28. Radaj D, Vormwald M. Advanced methods of fatigue assessment. 2013;9783642307.
29. Radaj D. State-of-the-art review on the local strain energy density concept and its relation to the J-integral and peak stress method. *Fatigue Fract Eng Mater Struct*. 2015;38(1):2-28.
30. Lazzarin P, Berto F. Some expressions for the strain energy in a finite volume surrounding the root of blunt V-notches. *Int J Fract.* 2005;135(1-4):161-185.
31. Lazzarin P, Berto F. From Neuber's elementary volume to Kitagawa and Atzori's diagrams: an interpretation based on local energy. *Int J Fract.* 2005;135:33-38.
32. Berto F, Lazzarin P, Gómez FJ, Elices M. Fracture assessment of U-notches under mixed mode loading: two procedures based on the 'equivalent local mode I' concept. *Int J Fract.* 2007;148(4):415-433.
33. Yosibash Z, Bussiba A, Gilad I. Failure criteria for brittle elastic materials. *Int J Fract.* 2004;125(3/4):307-333.
34. Lazzarin P, Sonsino CM, Zambardi R. A notch stress intensity approach to assess the multiaxial fatigue strength of welded tube-to-flange joints subjected to combined loadings. *Fatigue Fract Eng Mater Struct*. 2004;27(2):127-140.
35. Gómez FJ, Elices M, Berto F, Lazzarin P. A generalised notch stress intensity factor for U-notched components loaded under mixed mode. *Eng Fract Mech*. 2008;75(16):4819-4833.
36. Gómez FJ, Elices M, Berto F, Lazzarin P. Local strain energy to assess the static failure of U-notches in plates under mixed mode loading. *Int J Fract.* 2007;145(1):29-45.
37. Gómez FJ, Elices M, Berto F, Lazzarin P. Fracture of U-notched specimens under mixed mode: experimental results and numerical predictions. *Eng Fract Mech.* 2009;76(2):236-249.
38. Lazzarin P, Berto F, Ayatollahi MR. Brittle failure of inclined key-hole notches in isostatic graphite under in-plane mixed mode loading. *Fatigue Fract Eng Mater Struct*. 2013;36(9):942-955.
39. Lazzarin P, Lassen T, Livieri P. A notch stress intensity approach applied to fatigue life predictions of welded joints with different local toe geometry. *Fatigue Fract Eng Mater Struct*. 2003;26(1):49-58.
40. Berto F, Lazzarin P, Marangon C. Brittle fracture of U-notched graphite plates under mixed mode loading. *Mater Des.* 2012;41:421-432.
41. Livieri P, Lazzarin P. Fatigue strength of steel and aluminium welded joints based on generalised stress intensity factors and local strain energy values. *Int J Fract*. 2005;133(3):247-276.
42. Atzori B, Berto F, Lazzarin P, Quaresimin M. Multi-axial fatigue behaviour of a severely notched carbon steel. *Int J Fatigue.* 2006;28(5-6):485-493.
43. Berto F, Lazzarin P. Fatigue strength of structural components under multi-axial loading in terms of local energy density averaged on a control volume. *Int J Fatigue.* 2011;33(8):1055-1065.
44. Berto F, Lazzarin P. A review of the volume-based strain energy density approach applied to V-notches and welded structures. *Theor Appl Fract Mech.* 2009;52(3):183-194.
45. Ansys® academic research mechanical, release 19.1.
46. Remes H, Gallo P, Jelovica J, Romanoff J, Lehto P. Fatigue strength modelling of high-performing welded joints. *Int J Fatigue.* 2020;135:105555.

How to cite this article: Foti P, Berto F. Fatigue assessment of high strength welded joints through the strain energy density method. *Fatigue Fract Eng Mater Struct*. 2020;43:2694–2702. https://doi.org/10.1111/ffe.13336